

Development of a Two-Fluid Drag Law for
Clustered Particles using Direct Numerical
Simulation and Validation through Experiments
HBCU/MI Award DE-FE0007260 Review Meeting
Program Manager: Steven Seachman

Seckin Gokaltun¹ , Norman Munroe² , Shankar Subramaniam³

¹Applied Research Center

Florida International University, Miami, FL

²Mechanical and Materials Engineering

Florida International University, Miami, FL

³Mechanical Engineering

Iowa State University, Ames, IA

June 13, 2013

Technical Background

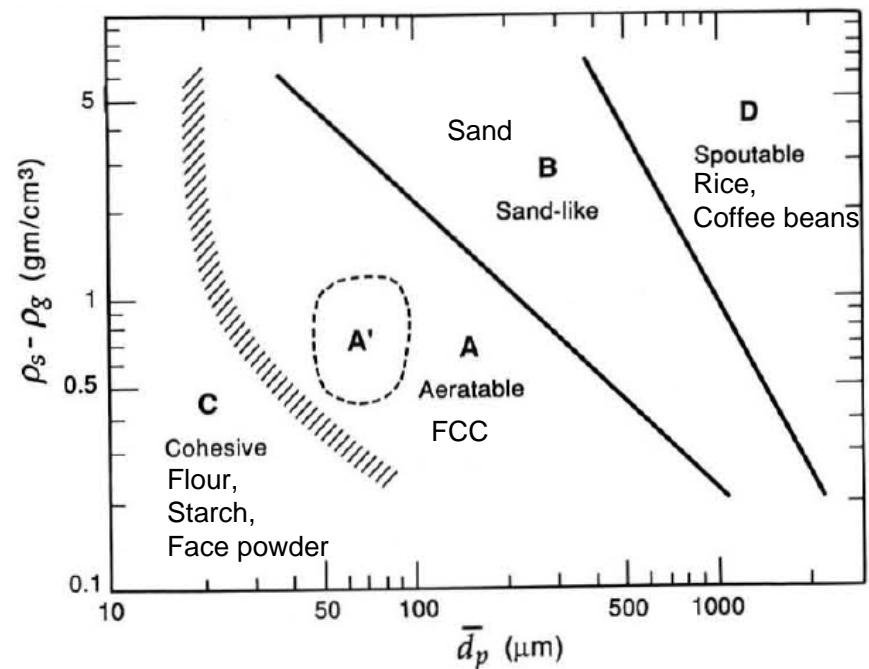
- ❑ Developers of gasifiers, combustors, chemical reactors, and owners of energy power plants are incorporating simulation in their design and evaluation processes to enhance process control and increase efficiency yield and selectivity.
- ❑ Several computational fluid dynamics (CFD) codes have been developed to simulate the hydrodynamics, heat transfer, and chemical reactions in fluidized bed reactors (MFIX, CFDLIB, etc.).
- ❑ Closure laws are required in the CFD simulations in order to capture the interaction between the gas and the solid phases in the system. For large scale simulations, a drag law is used in order to model the average interphase momentum transfer.
- ❑ Empirical correlations based on experiments by Ergun¹ and Wen-Yu² have been used frequently to calculate the drag force in dense and dilute flow regimes.

(1) Ergun, Chemical Engineering Progress, vol. 48, pp. 89-94, 1952.

(2) Wen and Yu, Chemical Engineering Progress Symposium Series, vol. 62, pp. 100-111, 1966.

Technical Background

- ❑ Particle-resolved direct numerical simulation (DNS) of flow past fixed particle assemblies^{3,4,5} yielded a drag relation that is more accurate than the Ergun and Wen-Yu correlations.
- ❑ These drag laws are applicable to suspensions where particles do not form clusters, and they have been useful in modeling the hydrodynamics of fluidized beds for Geldart B and D particles⁶.
- ❑ CFD simulation of fluidized beds with Geldart A particles remains a challenge because they fail to reproduce the pressure drop and bed expansion that are observed in experiments^{7,8}.
 - Formation of particle clusters significantly reduces the drag force.
 - The drag force is overestimated by standard drag laws.



(3) Hill et al., Journal of Fluid Mechanics, vol. 448, pp. 243-278, 2001.

(4) Beetstra et al., AIChEJ, vol. 53, pp. 489, 2007.

(5) Tenneti et al., International Journal of Multiphase Flow, 37, 1072-1092, 2011.

(6) van der Hoef et al., Annual Review of Fluid Mechanics, vol. 40, pp. 47-70, 2008.

(7) Wang et al. Chemical Engineering Science, vol. 64, no. 3, pp. 622-625, 2009.

(8) Wang, Ind. Eng. Res., vol. 48, no. 12, pp. 5567-5577, 2009.

Introduction

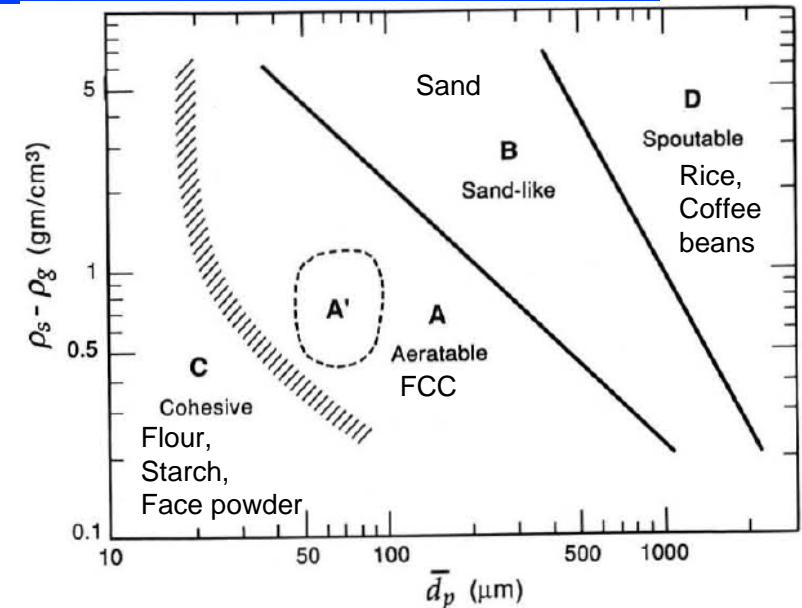
□ Geldart classification

➤ Geldart B particles

- ✓ Higher Re_m and St
- ✓ Uniform particle onfiguration

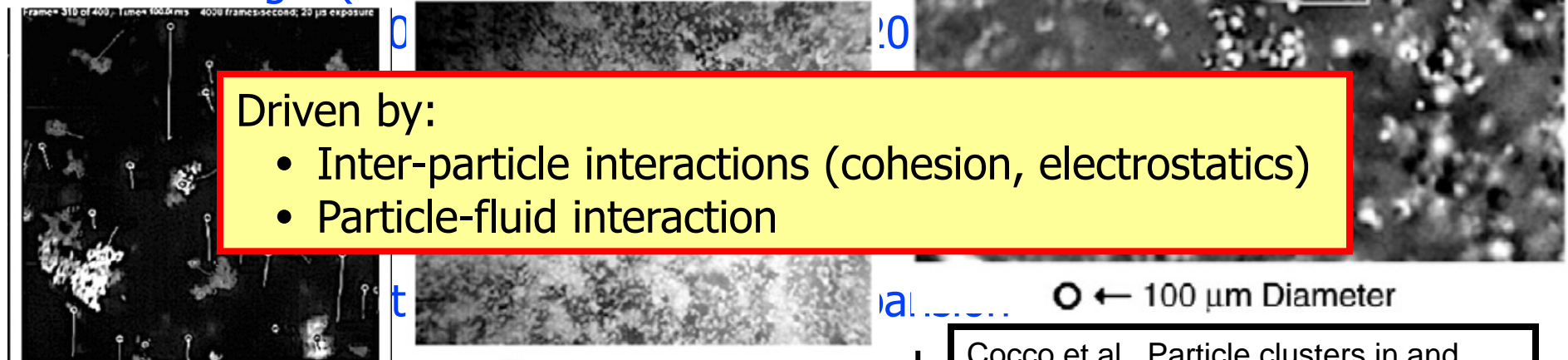
➤ Geldart A Particles

- ✓ Lower Re_m and St
- ✓ Formation of particle clusters



□ Plascoat™ 571 polyethylene ble for Geldart FCC catalyst in the bed

✓ Ergun(1952). Wen-Yu (1966). DNS:



Driven by:

- Inter-particle interactions (cohesion, electrostatics)
- Particle-fluid interaction

○ ← 100 μm Diameter

In the free board

○ ← 100 μm Diameter

In the fluidized bed

Cocco et al., Particle clusters in and above fluidized beds, Powder Technology, 2010

Technical Background

- ❑ Ad hoc approaches to account for the presence of particle clusters have been proposed (e.g., the Energy-minimizing Multi-Scale model) to modify the standard drag laws and these give improved simulation results in a limited fluidization regime.
- ❑ However, these ad hoc modifications do not have any predictive capability over the parameter range that is necessary for design optimization, nor do they provide insight into the fundamental multiphase flow physics.
- ❑ Therefore, a first-principles based approach is needed to quantify the mechanisms underlying particle clustering and their effect on the drag force.

Introduction

□ Current state-of-the-art clustered drag model used in CFD

➤ Energy minimization multi scale model⁽¹⁾ (EMMS)

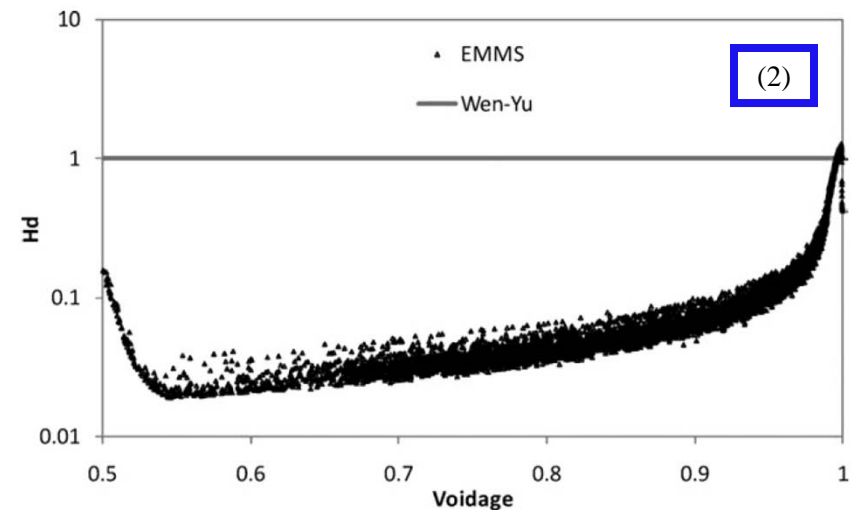
✓ Based on the minimum energy required for suspending and transporting dense particle regions

✓ Accounts for the effect of heterogeneous structures on drag based on *drag index*

$$\beta = \begin{cases} 150 \frac{\varepsilon_s (1 - \varepsilon_g) \mu_g}{\varepsilon_g d_p^2} + 1.75 \frac{\rho_g}{d_p} \varepsilon_s |\mathbf{v}_g - \mathbf{v}_s| & \varepsilon_g < 0.4 \\ \frac{3}{4} C_D \frac{\rho_g \varepsilon_g \varepsilon_s |\mathbf{v}_g - \mathbf{v}_s|}{d_p} \varepsilon_g^{-2.65} H_d & \varepsilon_g \geq 0.4 \end{cases}$$

Wen-Yu correlation

Drag index



➤ Not accounting for particle-particle interactions

⁽¹⁾ Li, J., Kwauk, M., Particle-Fluid Two-Phase Flow: the Energy-Minimization Multi-Scale Method; Metallurgy. Beijing: Industry Press, 1994.

⁽²⁾ Benyahia, S., Analysis of Model Parameters Affecting the Pressure Profile in a Circulating Fluidized Bed; AIChE Journal, 2012, 58 (2).

Motivation

- ❑ Physics-based model using PR-DNS
 - Explains physics
 - Results in a more accurate model
- ❑ Considering PR-DNS of a fixed clustered particle assembly
- ❑ Considering particle-particle cohesive forces

$$\tilde{F}_{p-p} = \frac{F_{p-p}}{F_{St}} = -\frac{Ad_p/(12x^2)}{3\pi d_p \mu_f |\langle \mathbf{W} \rangle|}$$

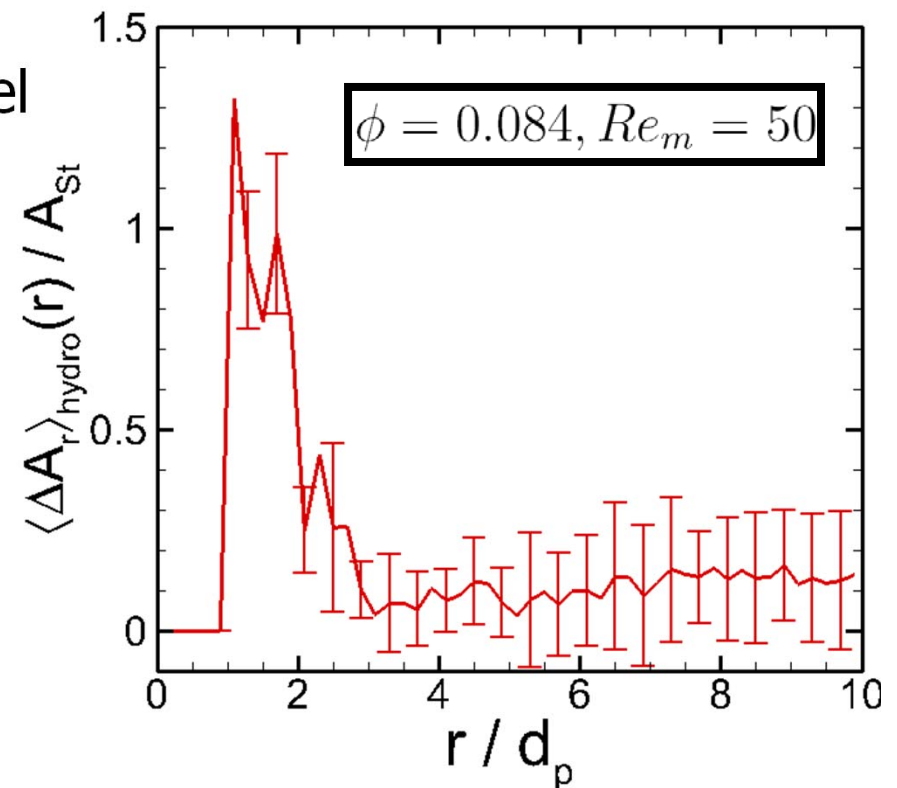
$$\tilde{F}_{p-p} = -\frac{Ha d_p}{36 d_0} \left(\frac{d_0}{x}\right)^2 \frac{Re_m}{(1-\phi)} \frac{T_{ss}^*}{|\langle \mathbf{W} \rangle|^2}$$

$$Ha^{**} = \frac{A}{\rho \pi d_p^2 d_0 T}$$

Measure of the cohesive potential to the characteristic kinetic energy

Particles remain as aggregates if the cohesive forces overcome the hydrodynamic forces at contact

Relative radial acceleration



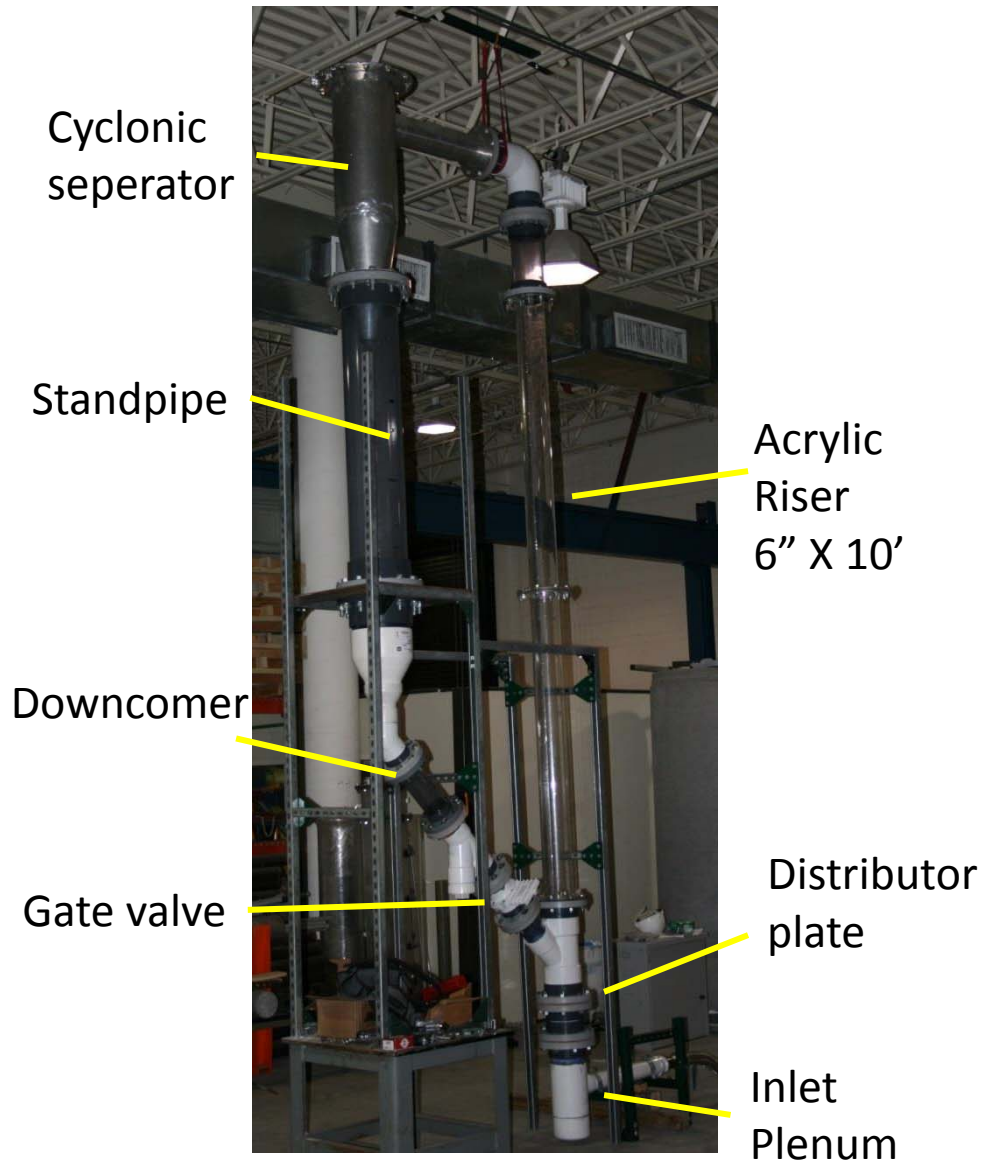
(*) Tenneti, S., Momentum, energy and scalar transport in polydisperse gas–solid flows using particle–resolved direct numerical simulations. PhD Thesis, Iowa State University, 2012.

(**) Eric Murphy, Iowa State University.

Technical Background

- ❑ The current research includes utilization of a combination of numerical and experimental approaches to provide detailed data necessary for validation and optimization purposes.
 - Experimental evaluation of particle clusters will be investigated using high speed imaging.
 - The drag law applicable to particle clustering in fluidized beds will be developed using direct numerical simulations.
 - Finally the developed drag law will be implemented in the MFIX software and the results will be validated against experimental data.

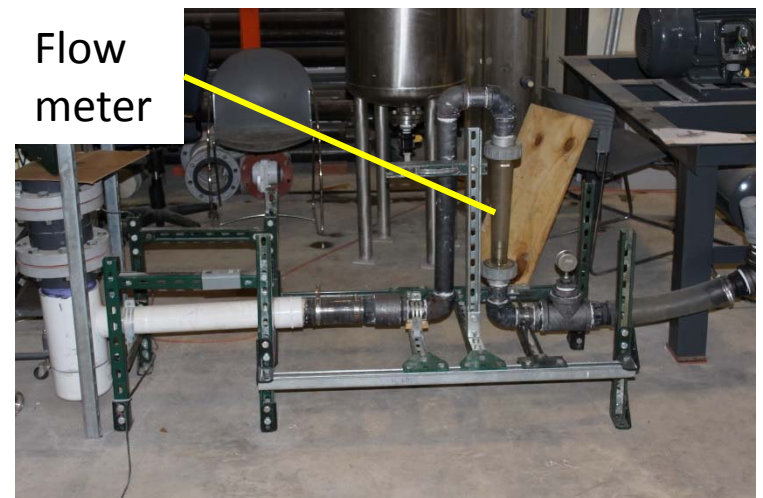
FIU Circulating Fluidized Bed



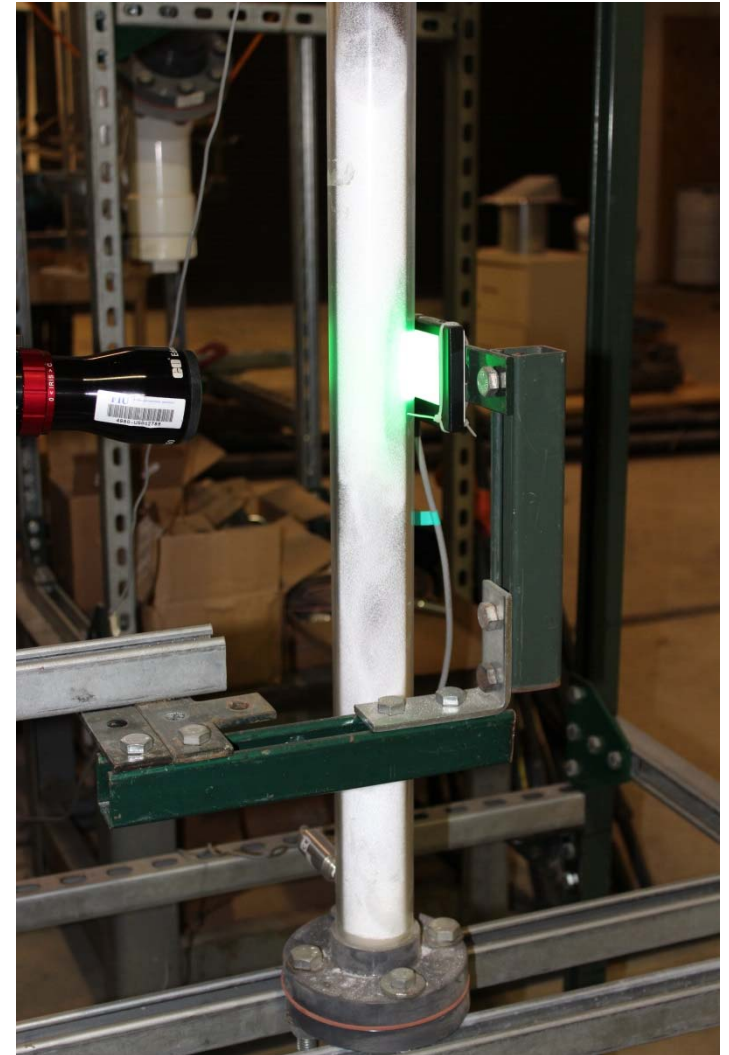
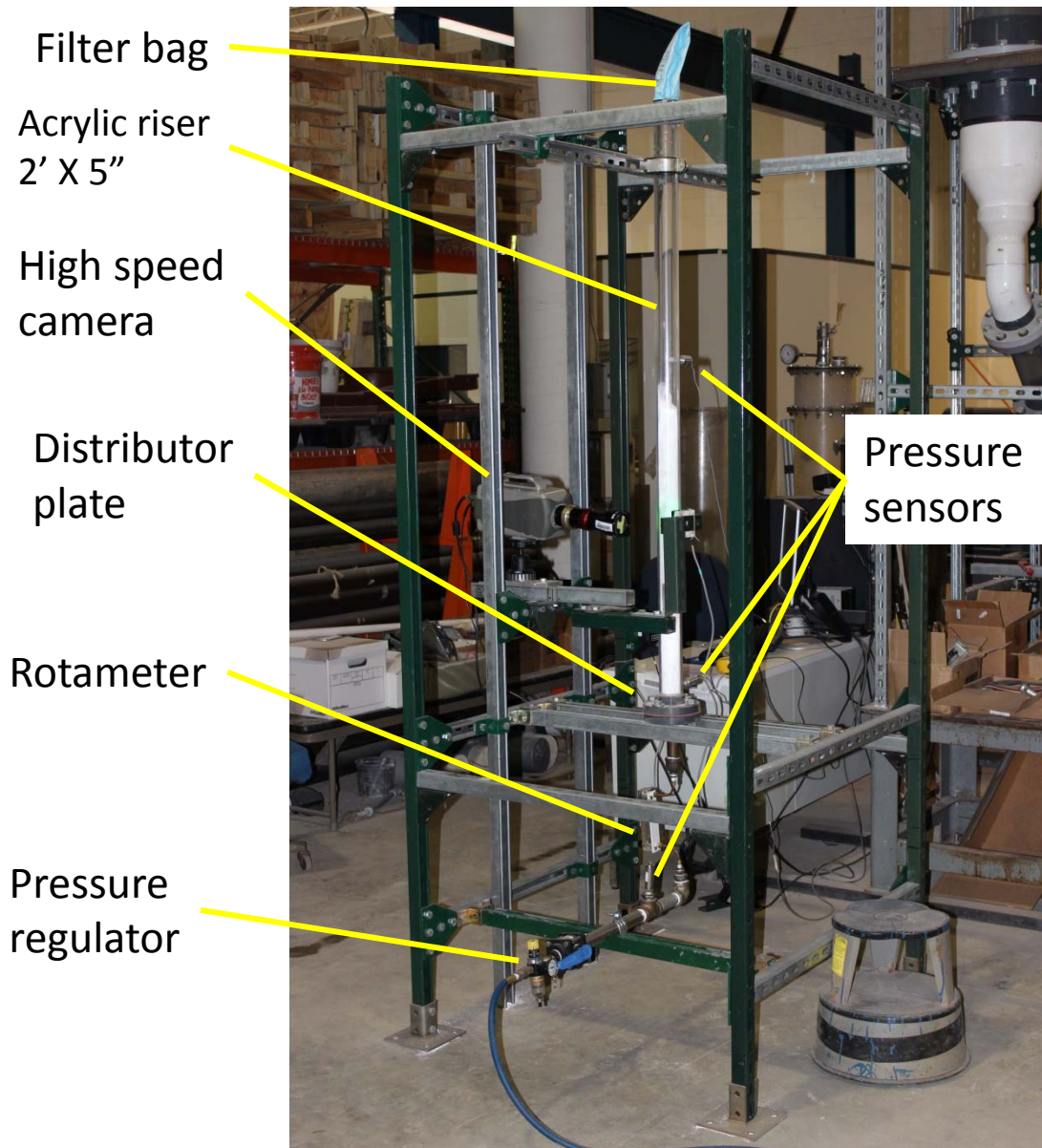
Roots Blower



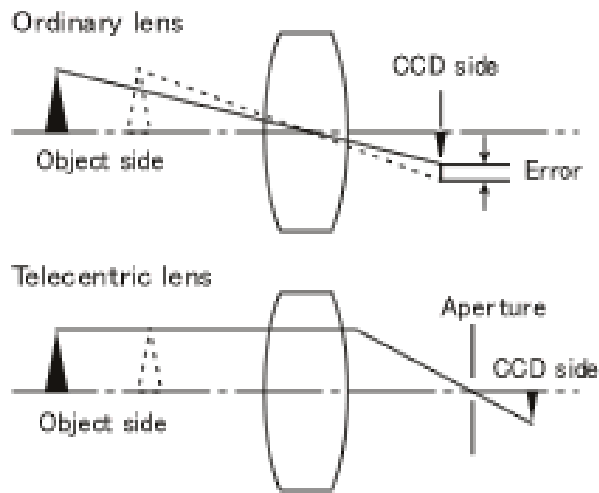
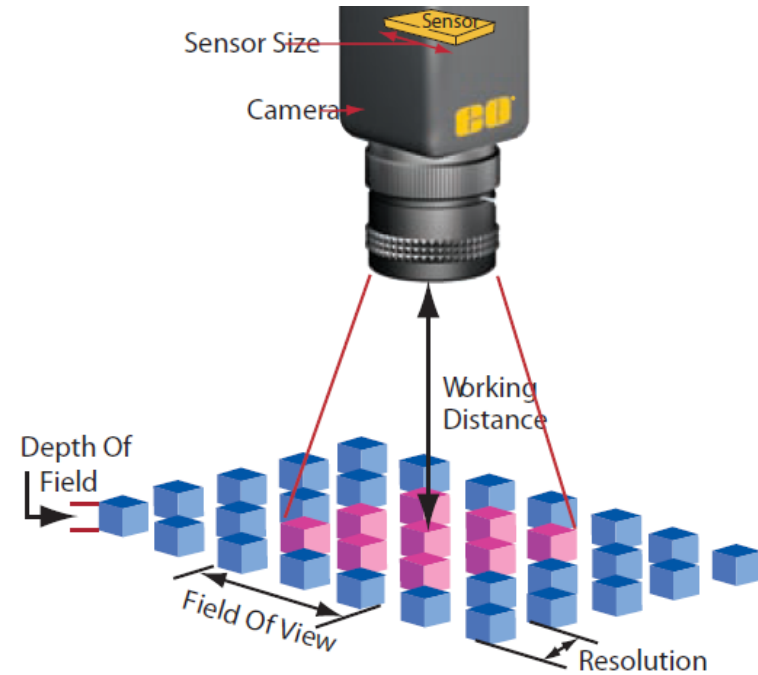
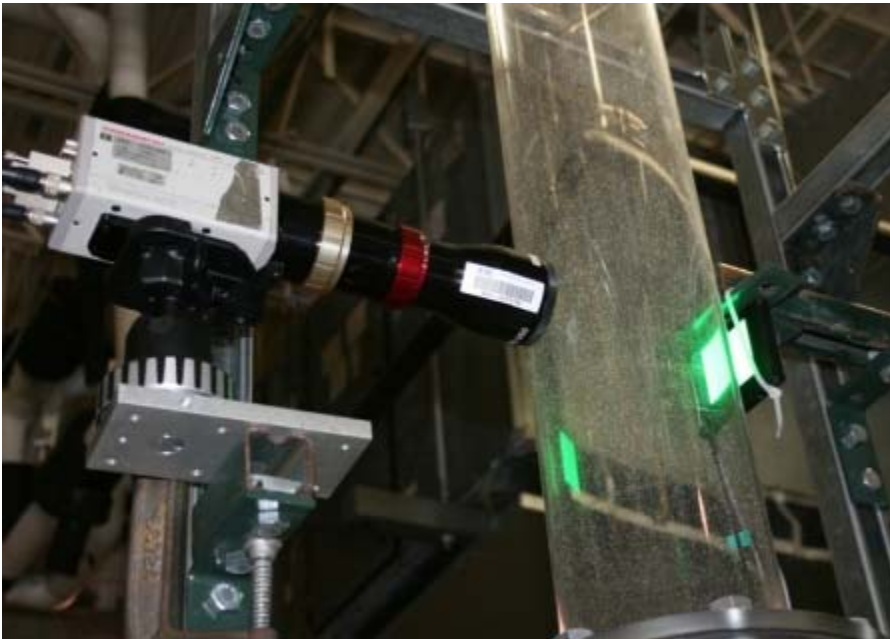
Flow meter



FIU BubblingBed



Experimental Approach

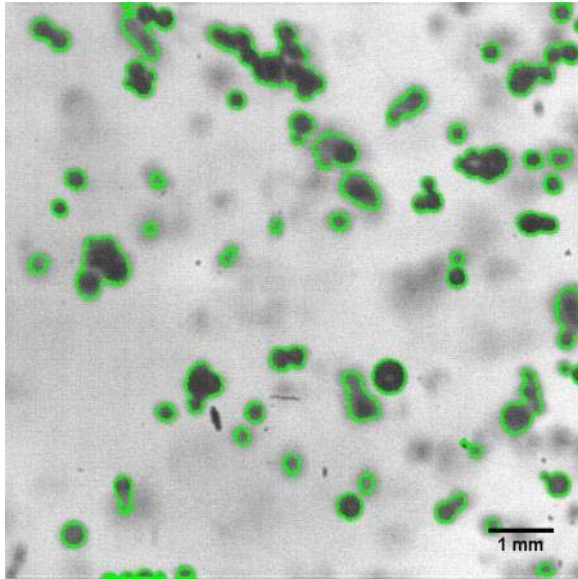


Telecentric Lens	Edmund Optics 55-350
Primary magnification	1X
Horizontal field of view	8.8 mm
Working distance	98 mm – 123 mm
Resolution (MTF Image Space @ F6)	>45% @ 40 lp/mm
Telecentricity	<.1°
Distortion	.5% Max
Depth of field (20% @ 20 lp/mm)	± 0.6mm at F12
Aperture (f/#)	F6 – F25

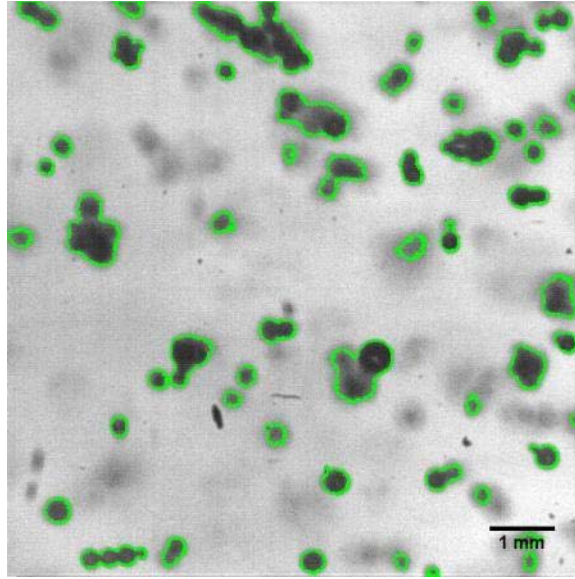
(11) S. Gokaltun, et al., Powder Technology, 220, pp. 98 –103, 2012.

Solid volume calculation

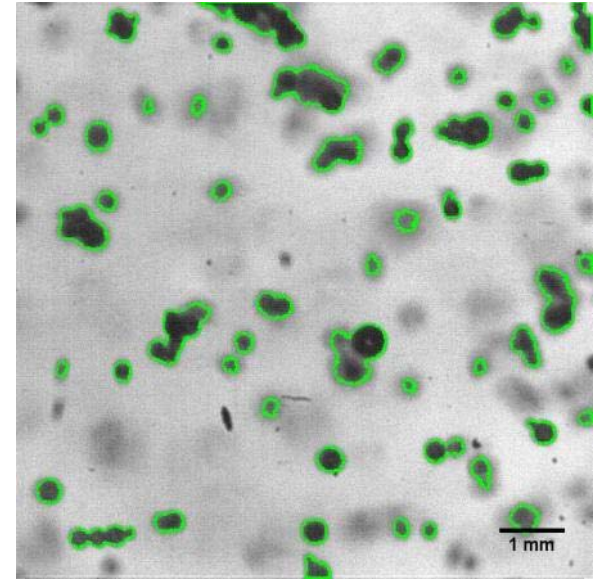
Frame 1



Frame 2



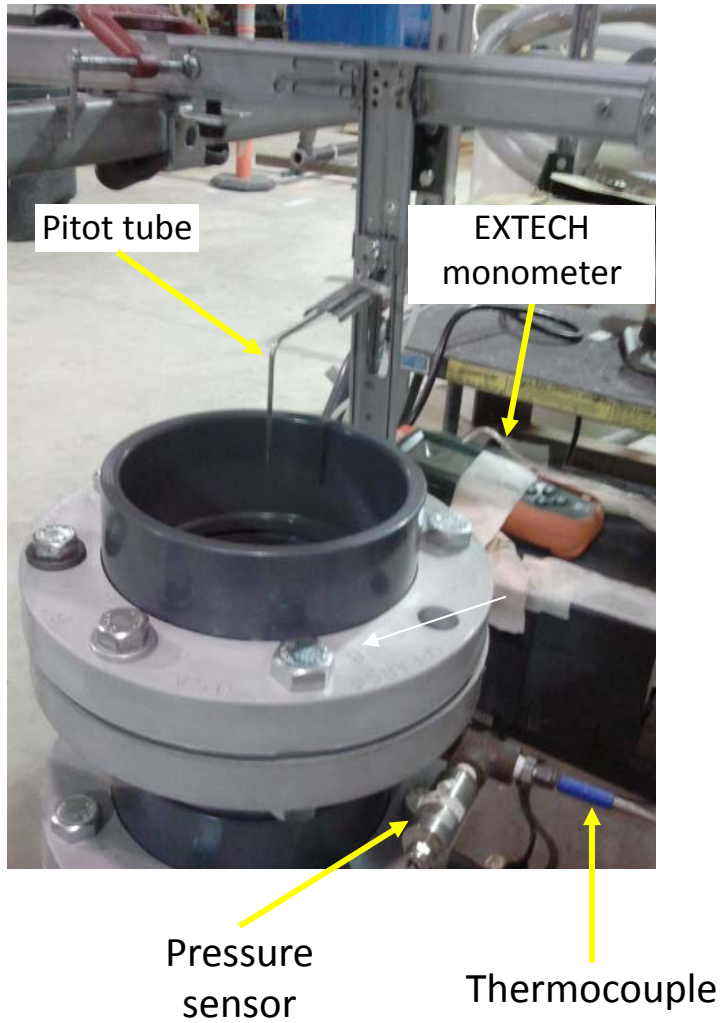
Frame 3



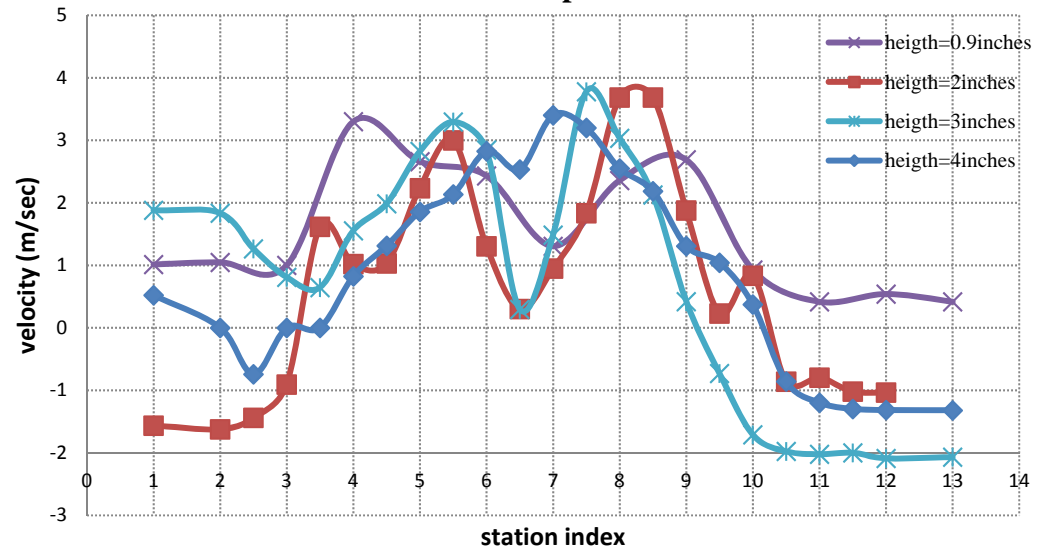
- ❑ Polystyrene particles:
 - $d_m=350\mu\text{m}$, $\rho_b=650\text{ kg/m}^3$
- ❑ Matlab Image Processing Toolkit used for frame by frame analysis.
- ❑ Telecentric lens (Edmund Optics Inc. 55 – 350)
 - horizontal field of view of 8.8mm
 - depth of field of 1mm
- ❑ Vision Research Phantom v5.0 (1024x1024 Sensor, 10 μs exposure time):
 - 3,800 pps @ 512 \times 512 pixels
 - 60,000 pps @ 256x32 pixels
 - 1024MB memory (1s of 1024 frames)

$$\varepsilon_s = \frac{\sum_i^n V_i}{Ah}$$

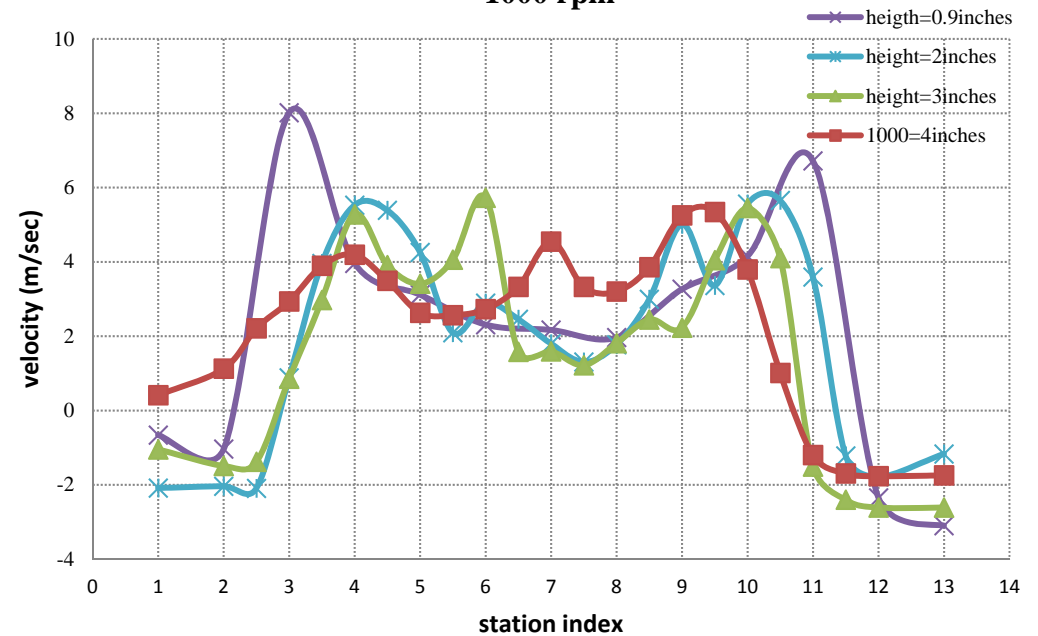
Velocity profile at inlet



500rpm



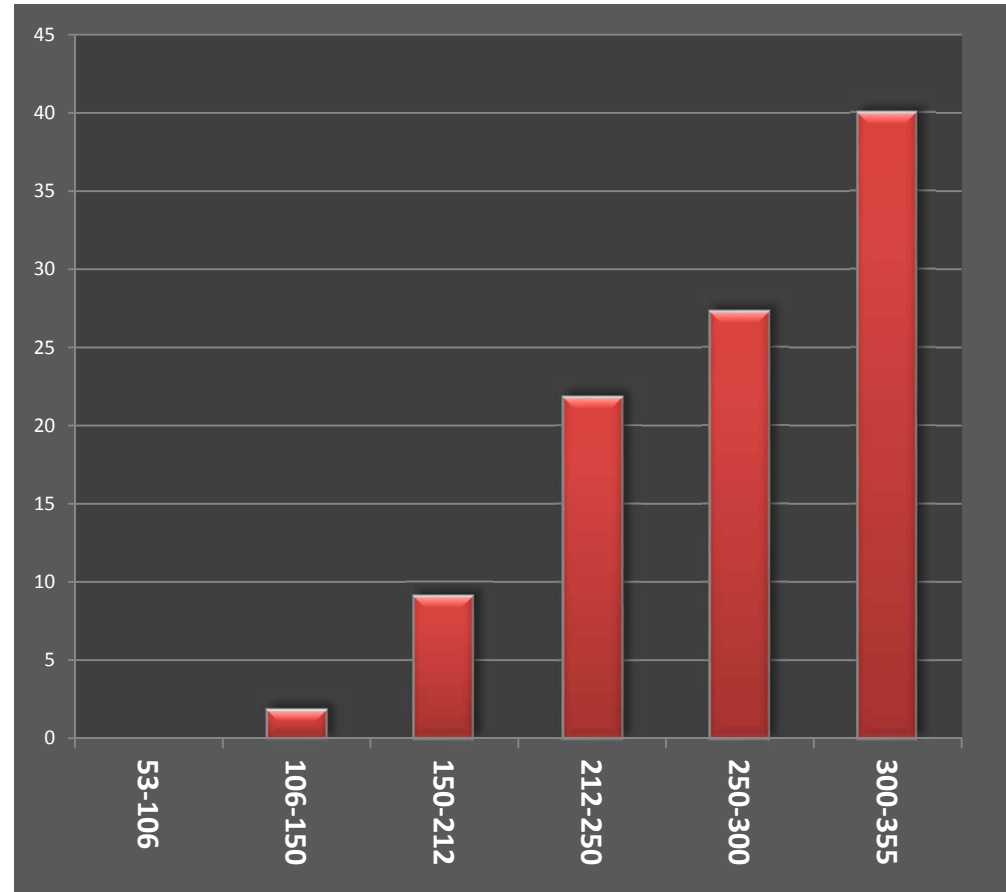
1000 rpm



Particle size analysis: Polystyrene



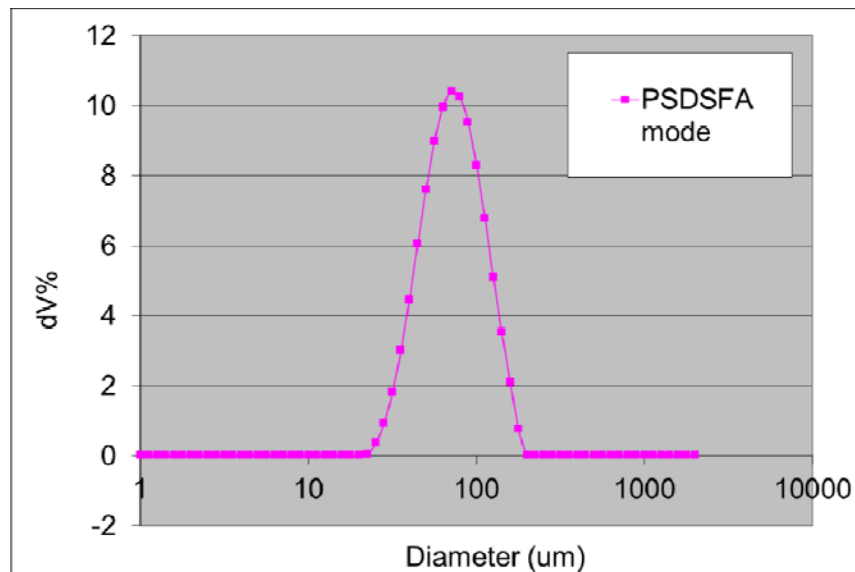
Shaker machine, implementing sieving mechanism to categorize particles



- Polystyrene particles
- mean diameter = 358 microns
- minimum diameter = 106 microns
- maximum diameter = 600 microns

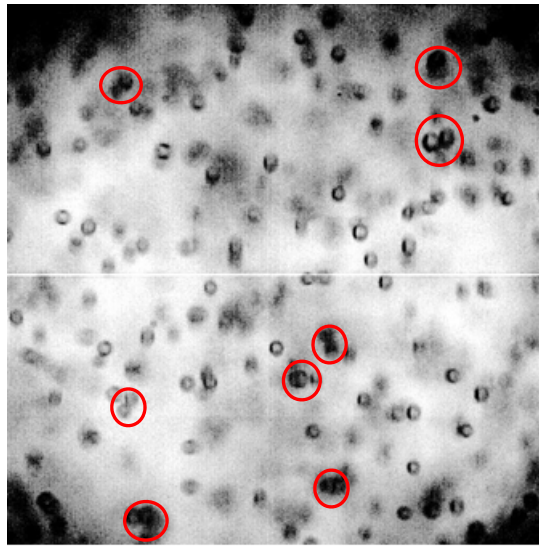
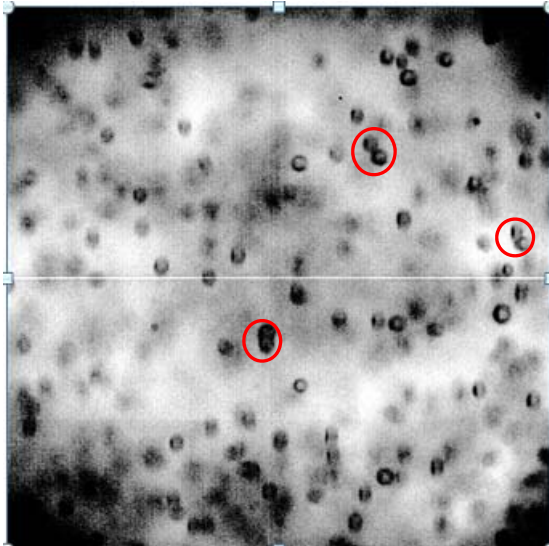
Particle size and chemical analysis: FCC

- Concerns with E&H Safety of spent FCC due to lead and hazardous content.
- Albemarle company has offered to do an X-ray Fluorescence analysis of the particles FIU has previously acquired to verify the information given in the MSDS.
- FIU has purchased a sampling thief and sent a representative sample of 250 ml of FCC to Albermarle for analysis.



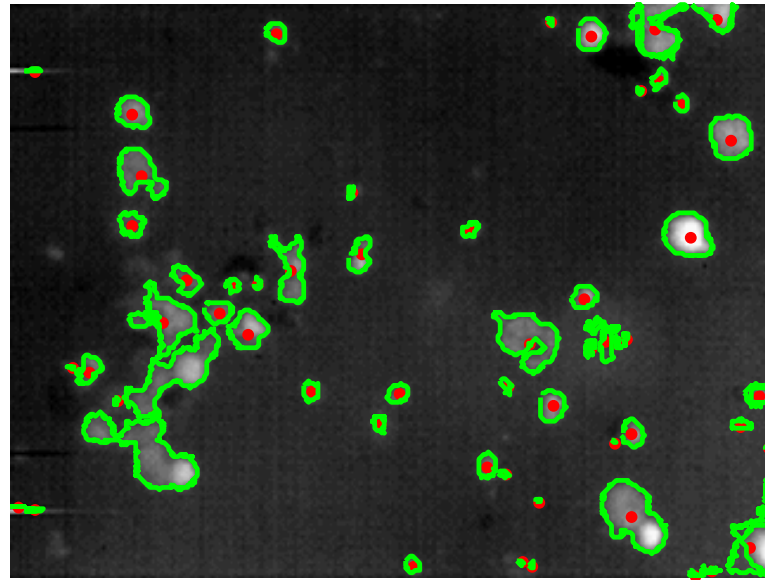
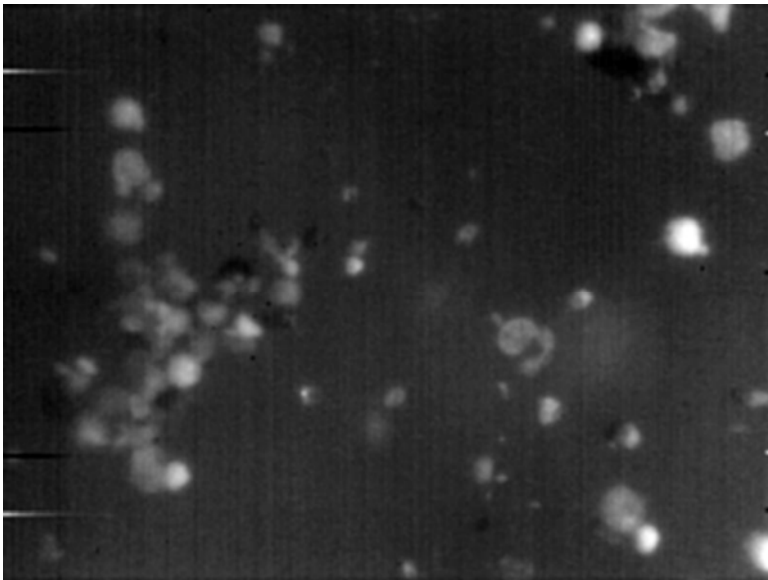
	XRF Analysis	MSDS	WT%
Sodium Oxide NA2O	0.644	0.2-1.5	WT%
Alumina AL2O3	54.23	20-75	WT%
Silica SIO2	41.54	25-80	WT%
Magnesia MGO	0.29		WT%
Barium Oxide BAO	0		WT%
Ferric Oxide FE2O3	0.61	0.2-2.0	WT%
Calcium Oxide CAO	0.11		WT%
Potassium Oxide K2O	0.06		WT%
Phosphorus pentoxide P2O5	0.46		WT%
Strontia SRO	0.01		WT%
Lanthanum oxide LA2O3	0.88		WT%
Neodymium Oxide ND2O3	0.02		WT%
Cerium Oxide CEO2	0.02		WT%
Praseodymium Oxide PR6O11	0.01		WT%
Titanium dioxide TIO2	0.86	0.1-3.0	WT%
Nickel(II) oxide NIO	1322		PPM
Vanadium Pentoxide V2O5	3323		PPM
Copper(II) oxide CUO	21	5-1000	PPM
BIO	0		PPM
Antimony trioxide SB2O3	0		PPM
Tin dioxide SNO2	0		PPM
Zirconium dioxide ZRO2	82		PPM
REO	0.93		WT%
ZNO	0.03		WT%
WO3	0		WT%
NF	0.9987		
	Equivalent Ni and V ppmw		
Ni	1039	45-7000	
V	1861	45-7000	

Image analysis of clusters



Images of polystyrene particles in $\frac{1}{4}$ (on left) and $\frac{1}{8}$ (on right) depth span of the acrylic pipe.

FCC cluster images obtained from Frank Shaffer are under analysis.



Characterization of Particle Clusters

□ Single-point quantities

➤ Solid-phase volume fraction

- ✓ Average number of particles in a volume

$$\phi = N_p \frac{\pi}{6} \left(\frac{d_p}{\mathcal{L}} \right)^3$$

➤ Radius of gyration tensor

- ✓ Anisotropy of particle clusters

$$R_{g,ij}^2 = \frac{1}{N_{cl}} \sum_{k=1}^{N_{cl}} (x_{k,i} - x_{cl,i})(x_{k,j} - x_{cl,j})$$

➤ Radius of gyration

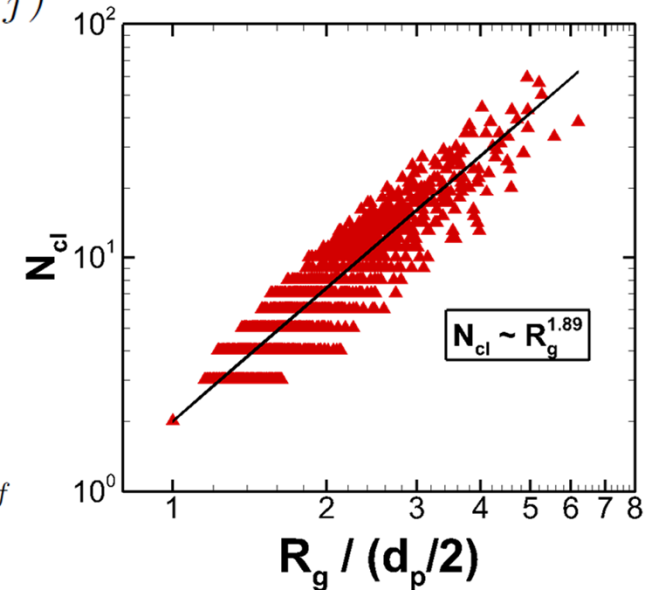
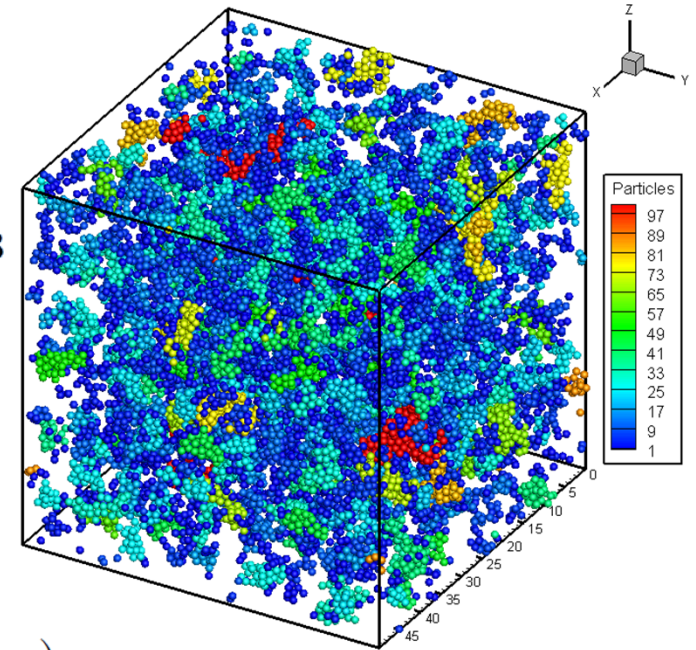
- ✓ Compactness of particle clusters

$$R_g = \left(R_{g,ii}^2 \right)^{1/2}$$

➤ Fractal dimension

- ✓ Geometrical Dimension of clusters

$$N_{cl} = k_0 \left(\frac{R_g}{d_p/2} \right)^{d_f}$$



Characterization of Particle Clusters

□ Two-point correlations

➤ Radial distribution function

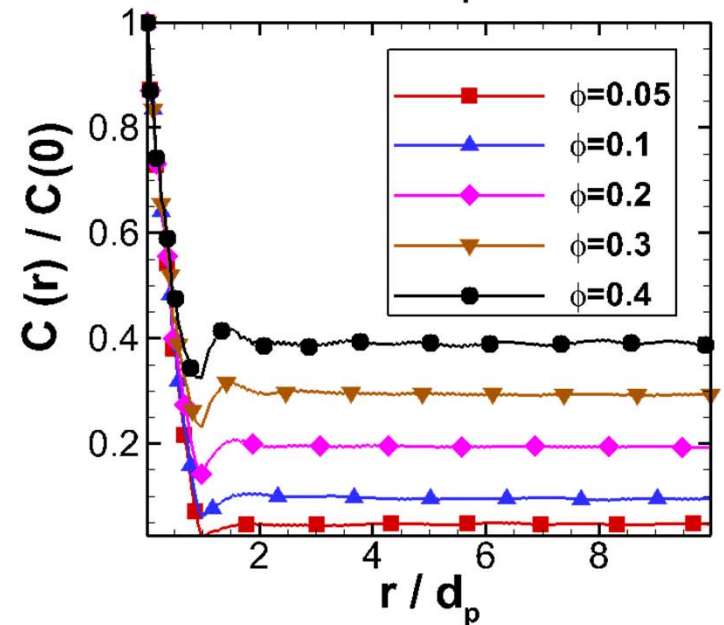
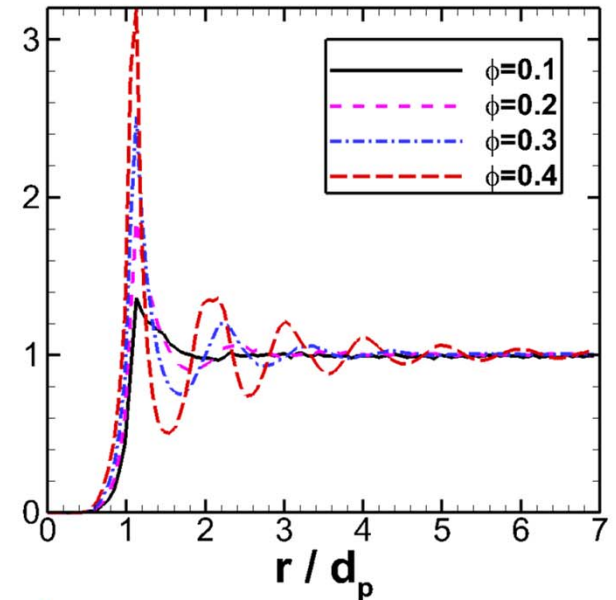
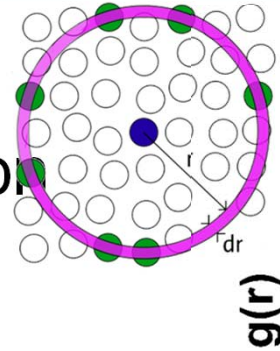
✓ Probability of finding
a particle at separation r

$$g(r) \equiv \frac{2}{N_p} \frac{N_r}{4\pi r^2 \delta r} \frac{V}{N_p}$$

➤ Spatial correlation function

✓ Probability of being in
solid phase at separation r

$$C(r) \equiv \langle I^{(p)}(\mathbf{x}) I^{(p)}(\mathbf{x} + \mathbf{r}) \rangle$$



Generation of Particle Clusters

□ Approach 1

- Using desired single-point and two-point quantities

 **Optimization problem**

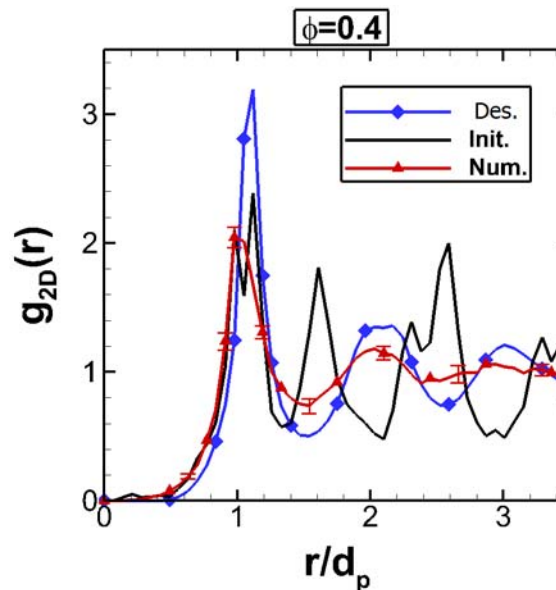
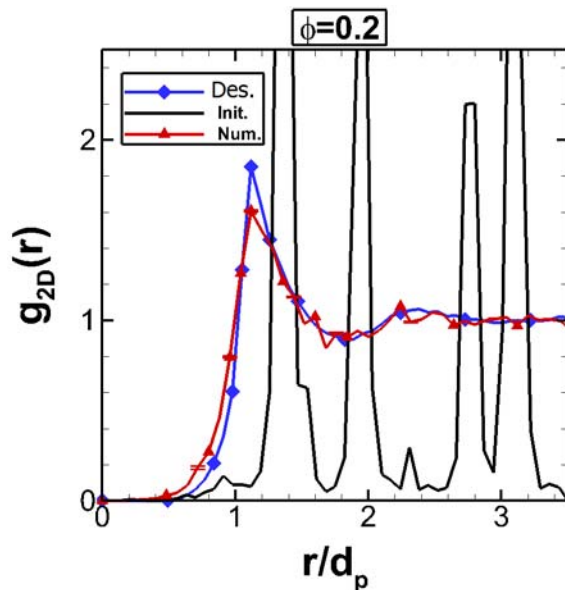
- Objective function

$$F \equiv \sum_{i=1}^M \gamma_i \left(f_i - f_i^{(\text{desired})} \right)$$

- Minimizing the function $\frac{\partial F}{\partial f_i} \rightarrow 0$

□ Simulated annealing (Kirkpatrick et al, 1983)

- Objectives: ϕ , $g(r)$



- Final configuration yields ϕ and $g(r)$ close to desired values
- Works well for lower volume fractions
- Still reasonable for higher volume fractions

Generation of Particle Clusters

□ Approach 2

➤ DEM of homogeneous colliding and cohesive particles

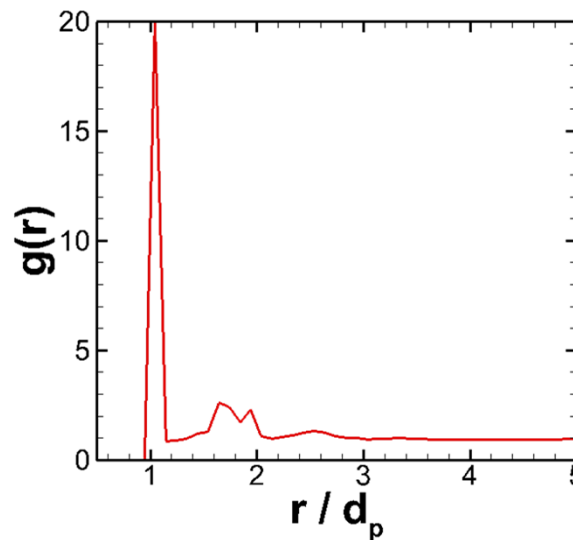
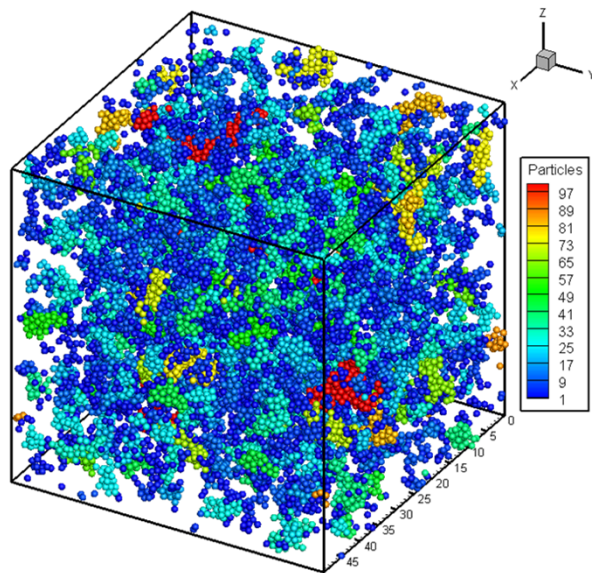
✓ Physics-based

✓ Higher computational cost

$$\begin{cases} Ha^{-1} \left(\frac{d_0}{d_p} \right)^2 \frac{d\tilde{\mathbf{V}}^{(i)}}{d\tilde{t}} + 1 = 0 \\ \frac{d\tilde{\mathbf{X}}^{(i)}}{d\tilde{t}} = \tilde{\mathbf{V}}^{(i)} \end{cases} \begin{cases} \tilde{t} = \frac{t\sqrt{T}}{d_0} \\ \tilde{\mathbf{X}}^{(i)} = \frac{\mathbf{x}^{(i)}}{d_0} \\ \tilde{\mathbf{V}}^{(i)} = \frac{\mathbf{v}^{(i)}}{\sqrt{T}} \\ Ha = \frac{A}{\rho\pi d_p^2 d_0 T} \end{cases}$$

➤ Selected system $\phi = 0.084$, $Ha = 0.8$, $d_0/d_p = 10^{-4}$, $L/d_p = 50$, $N = 20146$

➤ Simulation time $\tilde{t} = 7.04 \times 10^6$



- The simulation results in time-dependent particle clusters
- Appropriate sub-ensembles should be chosen for PR-DNS of gas-solid flows

Generation of Particle Clusters

□ Selection of particle sub-ensembles

➤ Cocco et al. (2010) *Powder Tech.*

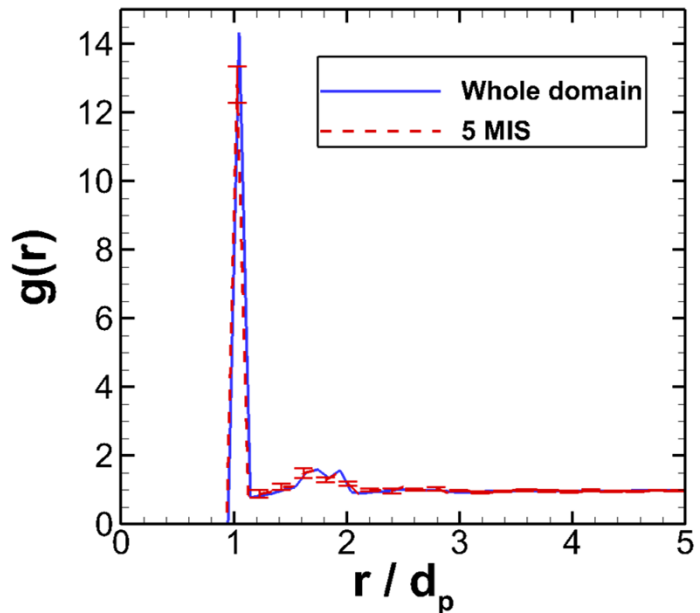
✓ Mean number of particles in a cluster is 26

✓ 75% of particles in clusters

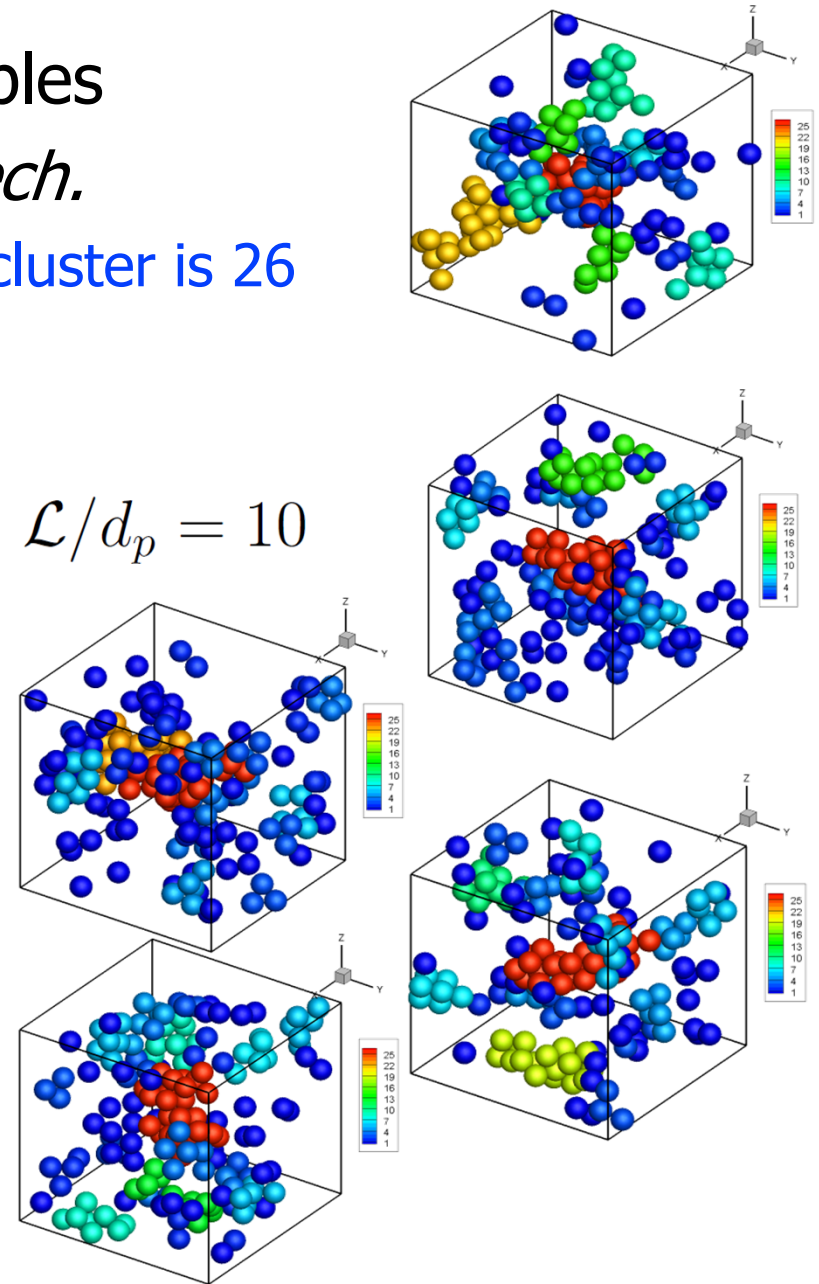
✓ 25% of particles as single

□ Choosing 5 sub-ensembles with $\mathcal{L}/d_p = 10$

➤ Consistent ϕ , $g(r)$



Sub-ensembles represent statistical properties of the whole domain



Numerical method

□ PUnReIBM $\partial_t \mathbf{u} + \nabla \cdot (\mathbf{u}\mathbf{u}) = -\frac{1}{\rho_f} \nabla p + \nu_f \nabla^2 \mathbf{u} + \mathbf{f}_u$

Particle-resolved

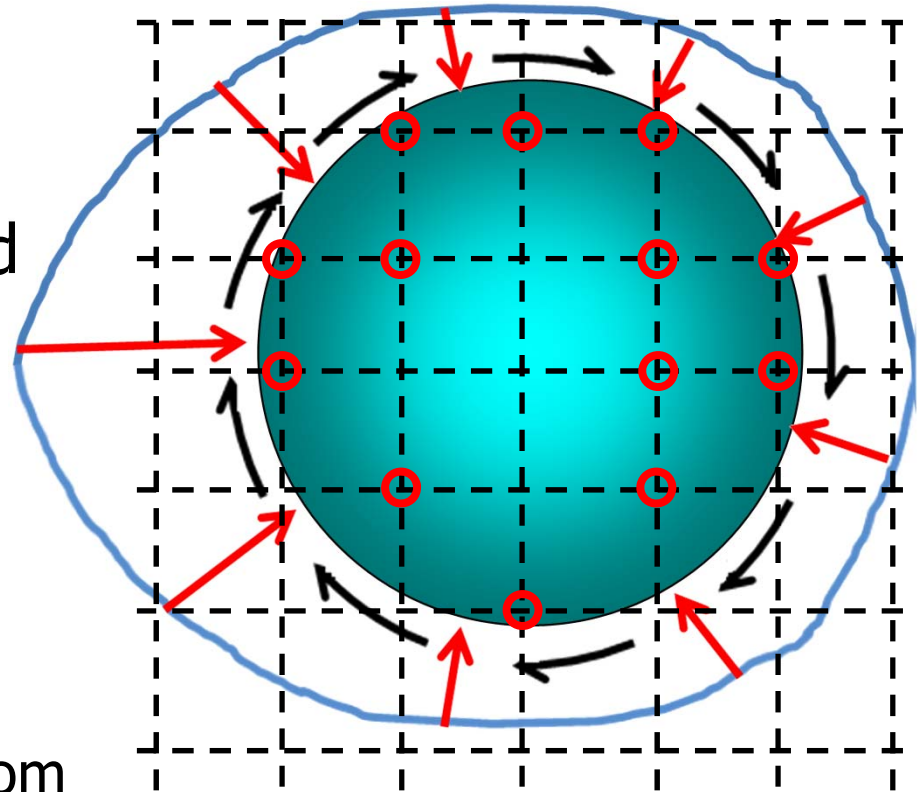
Uncontaminated-fluid

Reconcilable

Immersed Boundary Method

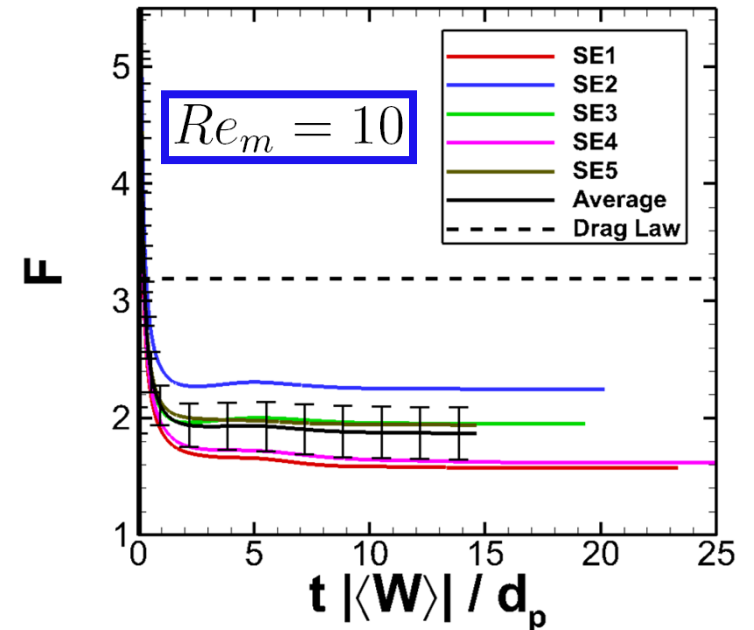
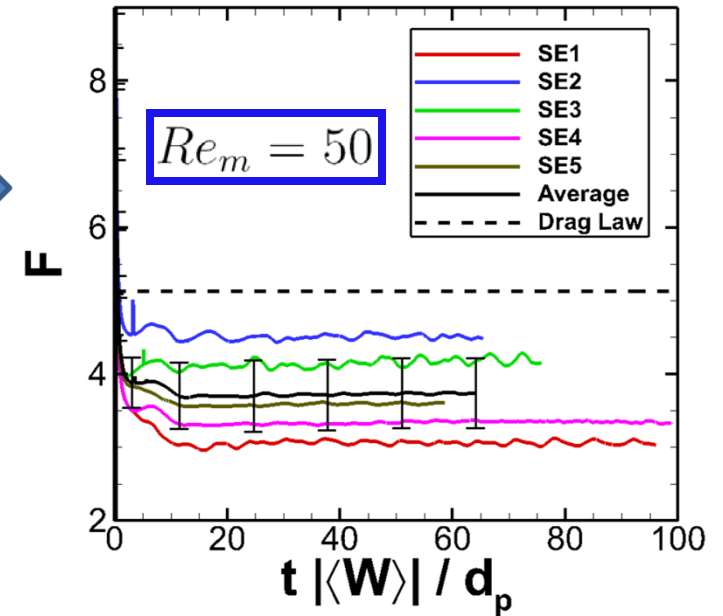
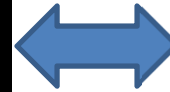
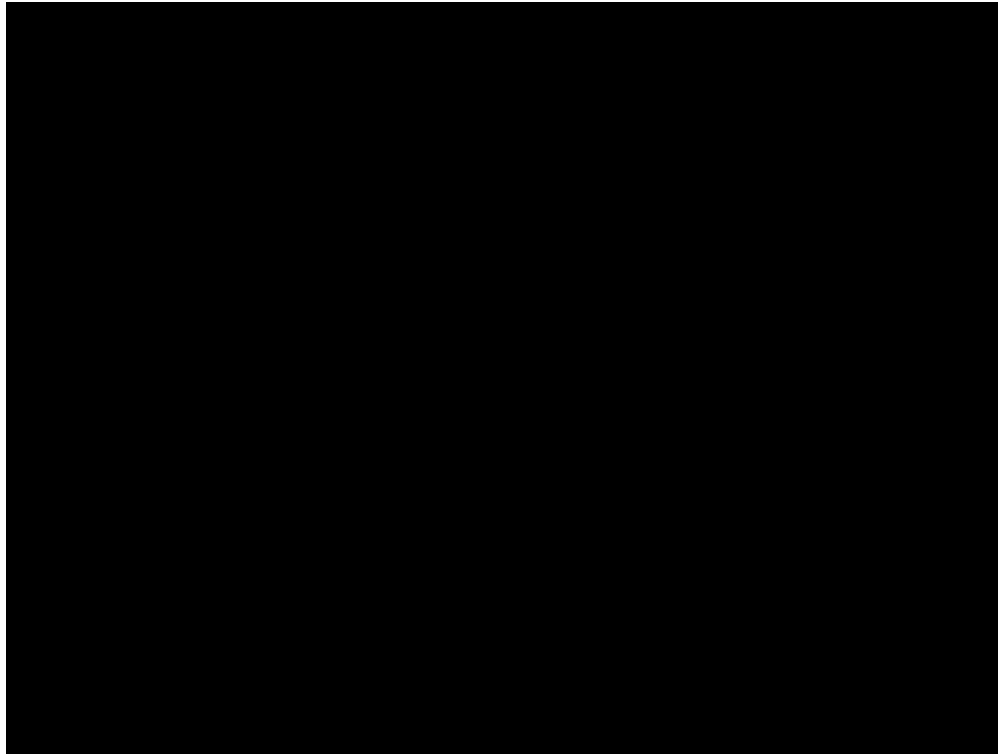
➤ Features

- ✓ Cartesian grid
- ✓ Continuum Navier-Stokes Solver
- ✓ No contaminations in fluid
- ✓ Drag computed directly from the stress
- ✓ Accurate and numerically convergent



Tenneti, S., Garg, R., Subramaniam, S., Drag law for monodisperse gas–solid systems using particle-resolved direct numerical simulation of flow past fixed assemblies of spheres. IJMF, 2011 (37) 1072-1092.

PR-DNS Results

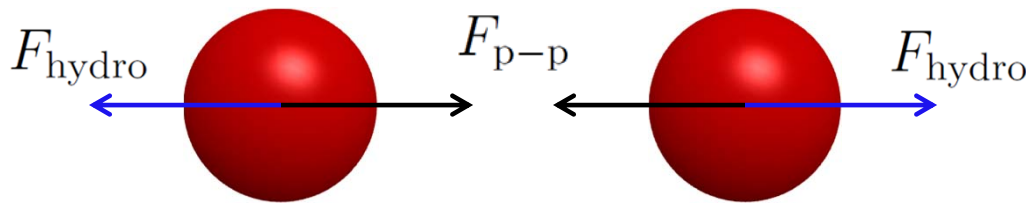


- Drag reduction is observed in clustered configurations
- Re_m is higher than the regime of interest
- Lower Re_m simulations are in progress

Proposed Drag Law

□ A function of

- A metric to identify criteria for formation of clusters
 - ✓ The ratio of relative hydrodynamic acceleration to that of particle-particle interaction such as cohesive forces



$$\frac{\langle \Delta A_r \rangle_{\text{hydro}}}{A_{\text{p-p}}}$$

- Solid-phase volume fraction and mean-slip Reynolds number

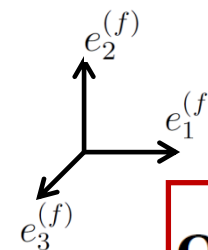
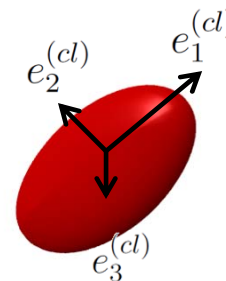
✓ Similar to uniform particle configuration drag law

$$\phi, Re_m$$

- Compactness of clusters R_g

- Anisotropy in clusters

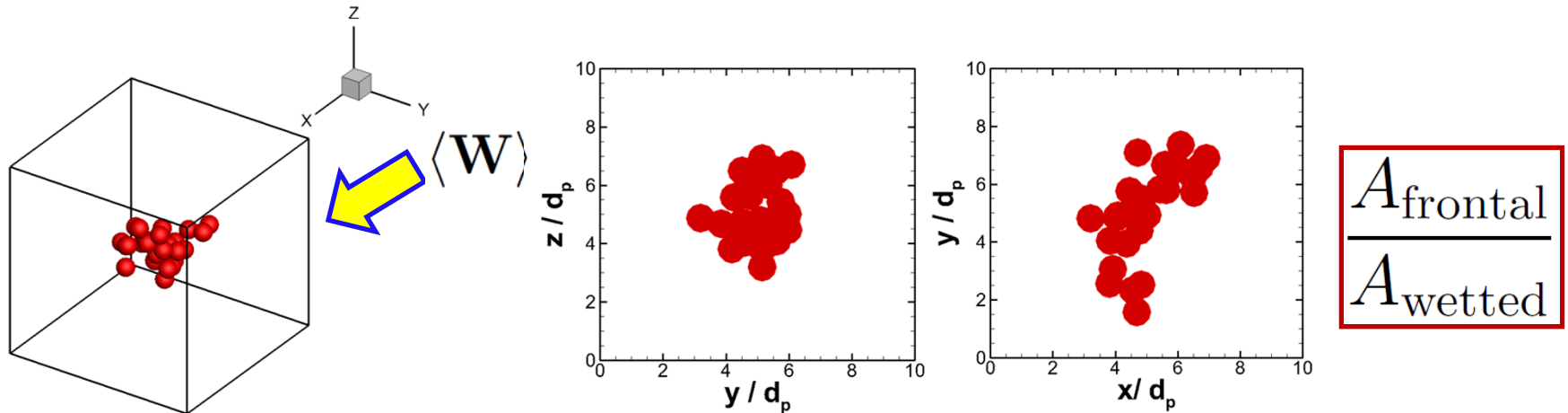
✓ Alignment of cluster principal axis and mean flow unit vector



$$\mathbf{e}^{(f)} \otimes \mathbf{e}^{(cl)}$$

Proposed Drag Law

- The ratio of frontal area to the wetted area of a cluster



- Tentative proposal for form of drag law might include a subset of parameters shown below:

$$F_{cl} = f \left(\frac{\langle \Delta A_r \rangle_{\text{hydro}}}{A_{p-p}}, \phi, Re_m, \frac{R_g}{d_p}, \mathbf{e}^{(f)} \otimes \mathbf{e}^{(cl)}, \frac{A_{\text{frontal}}}{A_{\text{wetted}}} \right)$$

- Depending on the regime of the flow, a linear combination of the uniform and clustered drag laws can be used

$$F = \omega F_{cl} + (1 - \omega) F_{uni}$$

□ Conclusion

- Simulated annealing method and DEM simulation of colliding and cohesive particles are used to produce particle clusters
- Particle clusters are characterized by single-point and two-point quantities that are useful for the general form of the clustered drag law
- Drag reduction is observed in gas-solid flows with clusters compared to uniform particle configurations

□ Future work

- Generation of particle configurations representing clusters observed in the regime of interest
- PR-DNS of gas-solid flows for selected clusters over the variable space associated with the regime of interest
- Proposing a drag law for particle clusters based on PR-DNS results

Technical Approach to Achieving the goals

□ DNS part

- Regeneration of 3D particle configuration using the experimental images
 - ✓ Simulated annealing approach
- Quantification of drag force from simulations
- Proposing a drag law that includes the clustering effects

$$F(\phi, Re_m, \sigma_\phi)$$

□ Validation

- Implement the model in MFIX
- Simulating a CFB configuration (setup from NETL)
- Validating the results with experiment

Questions and feedback?